Elastic proton scattering on ^{4}He at 156 MeV

V. Comparat, R. Frascaria, N. Fujiwara,* N. Marty, M. Morlet, P. G. Roos,† and A. Willis
Institut de Physique Nucléaire 91406, Orsay, France
(Received 17 March 1975)

The differential cross section for the proton ^{4}He elastic scattering at 156 MeV was measured in the angular range from 10° to 168°. An optical potential analysis with an exchange term is performed and extended to the 100 and 85 MeV data. Some of the impulse approximations are tested and a comparison is performed with a Glauber calculation.

[NUCLEAR REACTIONS ^{4}He(p,p), $E=156$ MeV measured $\sigma(\theta)$; optical potential analysis, impulse approximations tested.]

I. INTRODUCTION

Elastic proton scattering on light nuclei and especially on ^{4}He has been extensively studied at different energies as a test of the interaction mechanism.[1-9] Two approaches are generally used: the impulse approximation[10] and, for high energies, the Glauber approximation.[11] It is interesting to test and compare both treatments at an intermediate energy where the nucleon-nucleon interaction is well known.

Recent results at 85 MeV[2] and 100 MeV[3] show important backward angle cross sections. They were interpreted by an optical model analysis containing a Majorana exchange term. From a former experiment at 147 MeV,[5] this effect appeared to be less important at higher energies. Taking advantage of the liquid ^{4}He target described in the preceding paper (called I) we tried to extend the elastic scattering measurements to backward angles.

II. EXPERIMENTAL SETUP AND MEASUREMENTS

The intensity of the proton beam extracted from the Orsay synchrocyclotron incident on the target was monitored by an ionization chamber which has been normalized by reference to a Faraday cup.

Three different arrangements were used: for lab scattering angles ranging from 8.7° to 60° the protons were detected in the image plane of a magnetic analyzer by three telescopes consisting of three plastic scintillators in coincidence with a large plastic scintillator all located in the vacuum.[12] The three counters covered an over-all energy range of $\Delta E/E=1.25\%$. From 8.7° to 35° lab the angular apertures were horizontally ±0.25° and vertically ±0.5°. From 35° to 60° lab they were, respectively, ±0.5° and ±0.75°.

The region from 60° to 120° (74° to 133° c.m.) was measured with the $E\Delta E$ telescope described in I which covered a solid angle $\Delta\Omega=6.0\times10^{-4}$ sr. For scattering angles less than 90° lab a thin copper absorber was placed in front of the thick E plastic scintillator in order to limit the energy of the protons incident on the E detector to less than 100 MeV. The efficiency of the detector as a function of energy was obtained by measuring the pp elastic scattering on a liquid H target at various angles.

From 127.7° to 168° c.m. the p-^{4}He cross section was measured by detecting the recoil ^{4}He particles in the image plane of the magnetic analyzer. In order to minimize the detection of protons or deuterons with the same magnetic rigidity an absorber and a veto counter were placed behind the three telescopes. The thresholds of the three small plastic scintillators were raised and the ΔE spectrum on the second scintillator, common to the three telescopes, was measured. For angles larger than $\theta_{lab}=8.75°$ the α peak was completely separated from the proton and deuteron background. Six to seven measurements with different magnetic fields were necessary in order to cover the momentum spectrum of the recoil α particles.

In the experiment two different targets were used. For lab scattering angles less than 30°, a rectangular target 2 cm thick was set normal to the direction of the scattered particles in order to minimize the energy lost by the ^{4}He particles. For the other angles, the cylindrical target described in I was used.

For all angles smaller than 25° and at other angles for every second measurement, the background due to scattering on the Havar windows of the target was measured on an empty target with identical geometry.

The absolute cross section was obtained by measuring, in the geometry of the 35° to 60° lab

TABLE I. p-^{4}He differential cross section.

$\theta_{c.m.}$ (deg)	$(d\sigma/d\Omega)_{c.m.}$ (mb sr^{-1})	$\theta_{c.m.}$ (deg)	$(d\sigma/d\Omega)_{c.m.}$ (mb sr^{-1})
11.2	75.6 ± 2.19	101	0.0436 ± 0.0035
12.83	73 ± 2.14	106	0.038 ± 0.0031
16.0	52.2 ± 1.5	111	0.0345 ± 0.0025
19.2	39.2 ± 1.1	115.7	0.0287 ± 0.0027
22.4	26.8 ± 0.8	120.4	0.0263 ± 0.0019
25.6	15.9 ± 0.44	124.9	0.0180 ± 0.0018
28.7	10.4 ± 0.31	129.3	0.0130 ± 0.0012
31.9	7.17 ± 0.21	131.7	0.0117 ± 0.0011
38.1	4.9 ± 0.17	133.7	0.008 74 ± 0.001
44.3	2.97 ± 0.10	135.8	0.007 86 ± 0.0009
50.4	1.895 ± 0.064	139.5	0.0070 ± 0.009
56.5	1.16 ± 0.042	143.7	0.007 07 ± 0.0009
58.9	1.05 ± 0.035	147.7	0.0085 ± 0.0011
62.5	0.796 ± 0.026	151.8	0.0114 ± 0.0016
68.3	0.43 ± 0.014	155.8	0.0125 ± 0.0020
70.6	0.287 ± 0.010	160	0.017 ± 0.0025
74.0	0.222 ± 0.0074	162.5	0.0157 ± 0.0025
79.6	0.134 ± 0.0081	164	0.017 ± 0.0024
85.2	0.084 ± 0.0050	166	0.020 ± 0.0029
90.6	0.061 ± 0.004	168	0.0158 ± 0.0042
95.8	0.051 ± 0.0034		

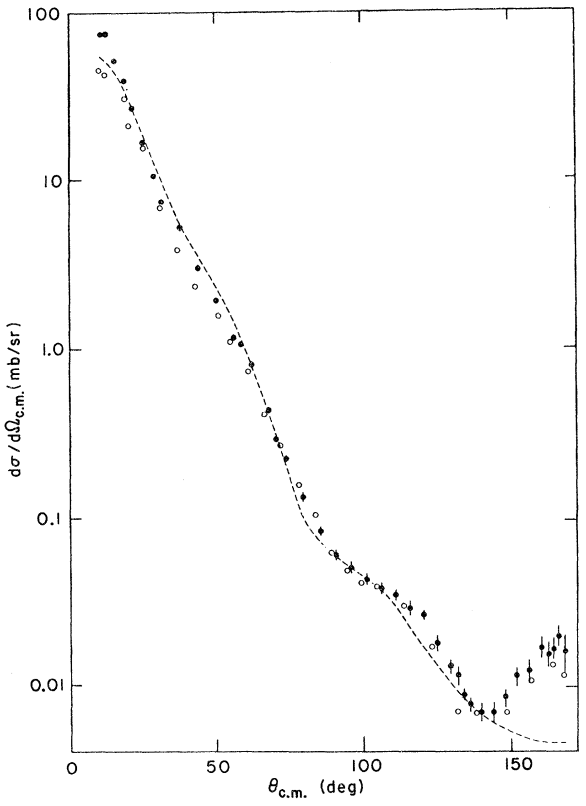

FIG. 1. p-^{4}He elastic differential cross section at 156 MeV. ● this experiment; ○ experimental points of Ref. 5; --- fit given by the optical potential Set a.

region, and with the same detectors, the proton-proton elastic cross section at $\theta_{lab} = 44.5°$ on a cylindrical H target. The pp cross section taken as a reference is $(d\sigma/d\Omega)_{90°\,c.m.} = 3.71 \pm 0.06$ mb sr^{-1}.[13]

The p-^{4}He differential cross section is given in Table I; the errors are statistical and normalization errors. An uncertainty of 5% on the absolute cross sections due to the uncertainty in the proton-proton reference cross section has not been included.

The angular distribution is given in Fig. 1 and compared to the results of Ref. 5. Small differences appear at the forward angles; at the backward angles ($\theta_{c.m.} > 140°$) our results are higher than those of Ref. 5. On the same figure is plotted the p-^{4}He elastic cross section given by the optical potential (Set a) (see Sec. III A).

III. INTERPRETATION OF THE EXPERIMENTAL RESULTS

A. Optical model analysis

The optical model analysis has been carried out with a modified version of the code JIBIV. The optical potential is written:

$$V(r) = V_c(r) - \frac{U_R}{1+e^{x_R}} - i\left(W_V - 4W_S \frac{d}{dx_I}\right)\frac{1}{1+e^{x_I}} + \left(\frac{\hbar}{m_\pi c}\right)^2 \left(U_{so} + iW_{so}\right)\frac{1}{r}\frac{d}{dr}\left(\frac{1}{1+e^{x_{so}}}\right)\vec{L}\cdot\vec{\sigma}$$

with

$$x_i = (r - r_i A^{1/3})/a_i \ .$$

Only pure volume absorption (Set a in the context of the optical model analyses performed on other nuclei at the same energy[14]) or pure surface absorption (Set b in the context of results at lower energies[2,3]) have been considered. To fix the spin-orbit parameters, the polarization measurements at 147 MeV[5] were included. Equivalent fits were obtained with both types of potentials. For Set a the total reaction cross section is $\sigma_R = 91.8$ mb and the volume integral per nucleon for the central part of the potential is $J/A = 187$ in agreement with the values obtained for other nuclei at the same proton energy.

To reproduce the rise in the backward cross section a Majorana exchange potential $V'(r)$ (see Refs. 2 and 3) has been added, viz.,

$$V'(r) = -(-1)^l U_E \frac{1}{1+\exp[(r-R_E)/a_E]}$$

with

$$R_E = r_E A^{1/3} \ .$$

TABLE II. Best sets of optical potential parameters (energies are given in MeV, lengths in fm).

Set	E_{lab}	U_R	r_R	a_R	W_V	W_S	r_I	a_I	V_{so}	W_{so}	r_{so}	a_{so}	U_E	r_E	a_E	r_C	χ^2/n
a	156	6.83	1.61	0.616	12.2	0	1.49	0.31	7.72	−5.53	0.79	0.266	0			1.36	23
b	156	5.58	1.89	0.396	0	15.16	0.818	0.465	9.69	−7.25	0.692	0.319	−3.4	0.426	0.420	1.36	20
c	100	13.078	1.533	0.102	0	8.774	1.336	0.398	7.53	−6.73	0.739	0.359	−10.24	0.127	0.714	1.36	4.8
d	85	15.26	1.634	0.226	0	2.20	1.83	0.92	4.21	−8.9	0.781	0.462	−10.88	0	0.879	1.36	5.6

Keeping the direct part of the potential from the preceding search, a search was performed on the parameters of the exchange potential, fitting the data only from the region of the minimum to the largest angle. Finally, all the parameters were left free for a last small adjustment of the fit over the full angular range.

To have some information on the dependence of the exchange potential as a function of the energy of the incoming proton the same analysis has been carried on the experimental results at 85 and 100 MeV.[2,3] At these energies there is some uncertainty in the spin-orbit part of the potential as no polarization measurements exist.

The best sets of parameters are given in Table II. The fits to the experimental results are given in Fig. 1 for Set a at 156 MeV (without exchange term), and on Fig. 2 for Set b at 156 MeV and Sets c and d at 100 and 85 MeV (with exchange term). The agreement with the parameters of Ref. 2 at 100 MeV is good except for the radius of the exchange potential which has been kept fixed by the authors.

Some general trends appear. The depth of the central direct and exchange potentials decreases when the energy of the incident proton increases, U_E being always smaller than U_R. The radius of V_R' is small and decreases with the energy while its thickness increases. The sum $r_E + a_E$ is nearly constant with energy and the shape of the exchange potential is more of a Gaussian than a Woods-Saxon type.

B. Impulse and Glauber approximations

The proton elastic scattering on ^{4}He has been treated in the framework of the impulse approximation given by Kerman, Mc Manus, and Thaler.[10] The first order approximation, where the coupling between the elastic channel and all other channels is neglected, is particularly suitable for ^{4}He; a detailed description of this treatment is given elsewhere.[15] The proton elastic scattering matrix for a nucleus of mass A is obtained by solving the Lippmann-Schwinger integral equation

$$T = AV + (A-1)\, VGT \qquad (1)$$

with

$$\langle \vec{k}' | V | \vec{k} \rangle = \langle \vec{k}' 0 | \tilde{t}^{nn} | \vec{k} 0 \rangle \ .$$

$|0\rangle$ is the ground state of ^{4}He, $\vec{k}$ and $\vec{k}'$ are the momenta of the incoming and outgoing proton, $\tilde{t}^{nn}$ is the free antisymmetrized nucleon-nucleon scattering matrix, and G is the proton-^{4}He propagator. The calculations are carried out with the Hamada-Johnston nucleon-nucleon interaction, excluding the Coulomb interaction. The ^{4}He nucleus is de-

scribed by a harmonic oscillator wave function with size parameter a. Two a values were used giving r.m.s. radii equal to 1.6 and 1.5 fm. The center of mass motion is accounted for by multiplying the form factor by $e^{q^2a^2/16}$, where q is the momentum transfer.

The validity of some approximations for momentum transfers less than 3 fm^{-1} (scattering angle less than 95° c.m.) has been tested by comparing with more exact calculations. In particular, it has been shown that:

(a) The kinematical Stern-Chamberlain approximation[16] can be used instead of the exact kinematics which require off-shell nucleon-nucleon matrices.

(b) The motion of the target nucleons in ^{4}He can be neglected as no sensitive difference appears when this motion is taken into account in an approximate manner.[15]

With these approximations the matrix T is then obtained by solving numerically Eq. (1) by the method proposed by Osborn.[17]

The calculations are presented in Fig. 3 (solid curves) for $\langle r^2\rangle^{1/2} = 1.6$ fm. They are compared to the experimental cross section data of the present experiment [Fig. 3(a)] and to the polarization results of Ref. 5 [Fig. 3(b)].

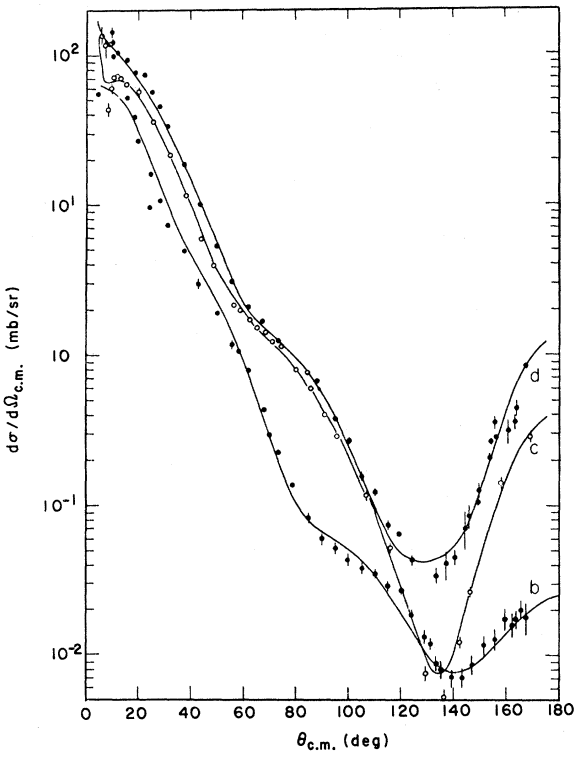

FIG. 2. p-^{4}He elastic differential cross sections at different energies and fits given by the optical potential Sets b at 156 MeV, c at 100 MeV, and d at 85 MeV.

Equation (1) is suitable for studying the convergence of a multiple scattering expansion. In Fig. 4 are plotted the first (T_1), second (T_2), and third (T_3) order terms of such an expansion where

$$T_1 = AV,$$

$$T_2 = T_1 + A(A-1)VGV,$$

$$T_3 = T_2 + A(A-1)^2 VGVGV.$$

It can be seen that the convergence of the Born

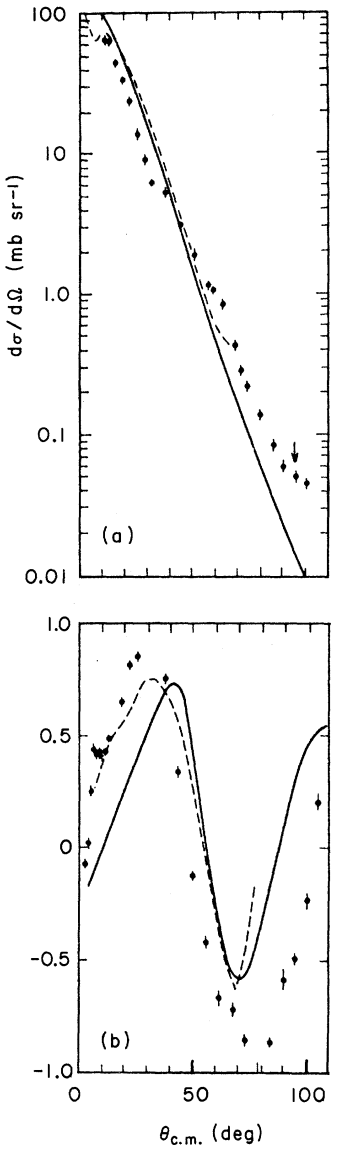

FIG. 3. p-^{4}He elastic differential cross section (a) and polarization (b) (the experimental points are from Ref. 5). — impulse approximation; --- Glauber approximation.

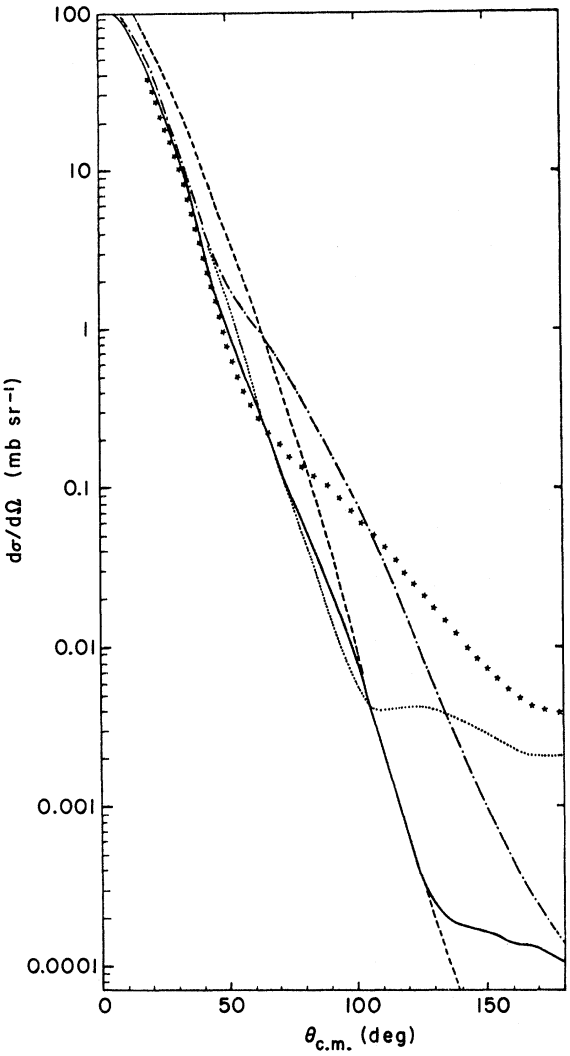

FIG. 4. Multiple scattering expansion of the first integral equation. — T; --- T_1; -·- T_2; ★★★ T_3; ... T_{IV}.

series is rather poor for large angles, but that T_3 is nearly identical to an exact calculation for $\theta_{c.m.}$ less than 65°. By analogy with the Glauber approximation[11] T_{IV} is the sum of the four first terms in which the principal part of the propagators has been taken equal to 0. It differs only slightly from the exact calculation in the range of validity ($\theta_{c.m.} < 90°$).

The experimental results were also compared to the usual Glauber calculations taken at the optical limit with the Hamada-Johnston nucleon-nucleon interaction.[18] ^{4}He is again described by a harmonic oscillator wave function with $\langle r^2 \rangle^{1/2} = 1.6$; no significant difference appears if the wave function proposed by Frosch *et al.*[19] is taken. In spite of all of the approximations and especially the "optical limit" which is valid for medium and heavy nuclei the Glauber approximation leads to results similar to those of the impulse approximation (see Fig. 3) and the general trend of the polarization is well given for $\theta_{c.m.} < 50°$.

IV. SUMMARY AND CONCLUSIONS

The proton differential elastic cross section on ^{4}He has been measured at 156 MeV in the angular range from 10° to 168° c.m. The results are well accounted for by an optical potential including an exchange term whose radius is much smaller than the radius of the direct term. In addition the depth of the exchange term decreases with increasing energy.

Different approximations of the impulse and the Glauber approximation were tested. They give a reasonably good account of the experimental results for scattering angles $\theta_{c.m.}$ less than 90°.

The authors are indebted to Dr. I. Brissaud for making the Glauber calculations for ^{4}He available to them.

*Permanent address: University of Kyoto, Kyoto, Japan.
†Permanent address: University of Maryland, College Park, Maryland 20742.

[1]G. E. Thompson *et al.*, Nucl. Phys. A142, 572 (1970).
[2]N. P. Goldstein, A. Held, and D. G. Stairs, Can. J. Phys. 48, 2629 (1970).
[3]L. G. Volta, P. G. Roos, N. S. Chant, and R. Woody, III, Phys. Rev. C 10, 520 (1974).
[4]W. Selove and J. M. Teem, Phys. Rev. 112, 1658 (1958).
[5]A. M. Cormack, J. N. Palmieri, N. F. Ramsey, and R. Wilson, Phys. Rev. 115, 599 (1959).
[6]O. Chamberlain *et al.*, Phys. Rev. 102, 1659 (1956).
[7]E. T. Boschitz *et al.*, Phys. Rev. C 6, 457 (1972).
[8]H. Palevsky *et al.*, Phys. Rev. Lett. 18, 1200 (1967).
[9]S. D. Baker *et al.*, Phys. Rev. Lett. 32, 839 (1974).
[10]A. K. Kerman, H. McManus, and R. M. Thaler, Ann. Phys. (N.Y.) 8, 551 (1959).
[11]R. J. Glauber, *Lectures in Theoretical Physics*, edited by W. E. Britten and L. G. Dunham (Interscience, New York, 1959), Vol. 1, p. 315.
[12]D. Bachelier *et al.*, Nucl. Phys. A126, 60 (1969).
[13]C. Caversazio and A. Michalowicz, J. Phys. (Paris) 21, 314 (1960).
[14]V. Comparat, R. Frascaria, N. Marty, M. Morlet, and A. Willis, Nucl. Phys. A221, 403 (1974).
[15]V. Comparat, Thèse d'Etat, Orsay, 1975 (unpublished).
[16]O. Chamberlain and M. O. Stern, Phys. Rev. 94, 666 (1954).
[17]T. A. Osborn, Nucl. Phys. A221, 211 (1973).
[18]I. Brissaud, L. Bimbot, Y. Le Bornec, B. Tatischeff, and N. Willis, Phys. Rev. C 11, 1537 (1975).
[19]R. F. Frosch, J. S. McCarthy, R. E. Rand, and M. R. Yearian, Phys. Rev. 160, 874 (1967).